Research Article | Vol. 26, No. 4 | 19 Feb 2018 | OPTICS EXPRESS 4512
Optics EXPRESS

Low-loss graded-index polymer crossed optical waveguide with high thermal resistance

KOHEI ABE,[1,*] YUTARO OIZUMI,[1] AND TAKAAKI ISHIGURE[2]

[1]*Graduate School of Science and Technology, Keio University, 3-14-1 Hiyoshi, Kohoku-ku, Yokohama, 223-8522, Japan*
[2]*Faculty of Science and Technology, Keio University, 3-14-1 Hiyoshi, Kohoku-ku, Yokohama, 223-8522, Japan*
**kouhei@keio.jp*
http://www.ishigure.appi.keio.ac.jp

Abstract: In this paper, crossed polymer waveguides with graded-index (GI) square cores are fabricated using the soft-lithography method. We experimentally demonstrate that the fabricated GI-core crossed waveguides exhibit a much lower insertion loss than conventional step index (SI)-core counterparts, which is almost independent of the cross angle. We also show in this paper that the crossed waveguides fabricated applying organic-inorganic hybrid resins show remarkably high thermal resistance compared to the waveguides fabricated utilizing an acrylate resin and a dopant system we previously reported.

OCIS codes: (130.5460) Polymer waveguides; (200.4650) Optical interconnects.

References and links

1. P. Pepeljugoski, J. Kash, F. Donay, D. Kuchta, L. Schares, C. Schow, M. Taubenblatt, B. J. Offrein, and A. Benner, "Low power and high density optical interconnects for future supercomputers," in *Optical Fiber Communication Conference* (Optical Society of America, 2010), paper OThX2.
2. A. F. Benner, M. Ignatowski, J. A. Kash, D. M. Kuchta, and M. B. Ritter, "Exploitation of optical interconnects in future server architectures," IBM J. Res. Develop. **49**(4.5), 755–775 (2005).
3. F. E. Doany, C. L. Schow, B. G. Lee, R. A. Budd, C. W. Baks, C. K. Tsang, J. U. Knickerbocker, R. Dangel, B. Chan, H. Lin, C. Carver, J. Haung, J. Berry, D. Bajkowski, F. Libsch, and J. A. Kash, "Terabit/s-class optical PCB links incorporating 360-Gb/s bidirectional 850 nm parallel optical transceivers," J. Lightwave Technol. **30**(4), 560–571 (2012).
4. R. C. A. Pitwon, K. Wang, J. Graham-Jones, I. Papakonstantinou, H. Baghsiahi, B. J. Offrein, R. Dangel, D. Milward, and D. R. Selviah, "FirstLight: Pluggable optical interconnect technologies for polymeric electro-optical printed circuit boards in data centers," J. Lightwave Technol. **30**(21), 3316–3329 (2012).
5. N. Bamiedakis, A. Hashim, R. V. Penty, and I. H. White, "A 40 Gb/s optical bus for optical backplane interconnections," J. Lightwave Technol. **32**(8), 1526–1537 (2014).
6. N. Bamiedakis, J. Beals, R. V. Penty, I. H. White, J. V. DeGroot, and T. V. Clapp, "Cost-effective multimode polymer waveguides for high-speed on-board optical interconnects," J. Quantum Electron. **45**(4), 415–424 (2009).
7. T. Sakamoto, H. Tsuda, M. Hikita, T. Kagawa, K. Tateno, and C. Amano, "Optical interconnection using VCSELs and polymeric waveguide circuits," J. Lightwave Technol. **18**(11), 1487–1492 (2000).
8. F. Betschon, M. Michlerb, D. Craiovanc, M. Halter, K. Dietrichb, J. Kremmelb, J. F. M. Gmür, and S. Paredes, "Mass production of planar polymer waveguides and their applications," Proc. SPIE **7607**, 76070M (2010).
9. A. Fujii, T. Suzuki, K. Shimizu, K. Yatsuda, M. Igusa, S. Ohtsu, and E. Akutsu, "A novel fabrication technology of a polymer optical waveguide and its application," Proc. SPIE **6775**, 677506 (2007).
10. T. Ishigure, K. Shitanda, and Y. Oizmi, "Index-profile design for low-loss crossed multimode waveguide for optical printed circuit board," Opt. Express **23**(17), 22262–22273 (2015).
11. B. W. Swatowski, C. M. Amb, M. G. Hyer, R. S. John, and W. K. Weidner, "Graded index silicone waveguides for high performance computing," in *Proceedings of IEEE Optical Interconnect Conference* (IEEE, 2014), pp. 133–134.
12. K. Kitazoe, A. Horimoto, K. Moriya, R. Kinoshita, K. Choki, and T. Ishigure, "Ultra low crossing loss meshed waveguide based on polynorbornene for backplane architecture," in *Proceedings of IEEE Optical Interconnect Conference* (IEEE, 2015), pp. 28–29.
13. K. Soma and T. Ishigure, "Fabrication of a graded-index circular-core polymer parallel optical waveguide using a microdispenser for a high-density optical printed circuit board," IEEE J. Sel. Top. Quantum Electron. **19**(2), 3600310 (2013).

#314608 https://doi.org/10.1364/OE.26.004512
Journal © 2018 Received 29 Nov 2017; revised 25 Jan 2018; accepted 26 Jan 2018; published 12 Feb 2018

Optics EXPRESS

14. R. Houbertz, V. Satzinger, V. Schmid, W. Leeb, and G. Langer, "Optoelectronic printed circuit board: 3D structures written by two-photon absorption," Proc. SPIE **7053**, 70530B (2008).
15. T. Ishigure and Y. Nitta, "Polymer optical waveguide with multiple graded-index cores for on-board interconnects fabricated using soft-lithography," Opt. Express **18**(13), 14191–14201 (2010).
16. K. Abe and T. Ishigure, "Fabrication for low loss graded-index polymer crossed optical waveguide using the soft-lithography method," in *Proceedings of IEEE Photonics Conference* (IEEE, 2016), pp. 753–754.
17. H. Nawata, "Organic-inorganic hybrid material for on-board optical interconnets and its application in optical coupling," in *Proceedings of IEEE CPMT Symposium Japan* (IEEE, 2013), pp. 121–124.
18. H. Nawata, T. Nagasawa, S. Tadokoro, K. Yasui, D. A. Sahade, T. Ishigure, S. Yoshida, Y. Saito, and K. Yasuhara, "Organic-inorganic hybrid material, "SUNCONNECT®" for optical interconnects," in *Proceedings of IEEE CPMT Symposium Japan* (IEEE, 2015), pp. 126–129.

1. Introduction

The trends in cloud computing technologies have accelerated the growth of the data rates for datacenter networks and high-performance computing (HPC) systems over the last couple of years [1]. To sustain the capacity of the datacenters, the data processing speed in the servers is required to increase continuously while maintaining low power consumption. Therefore, optical interconnect technologies have drawn much attention because they can realize high bandwidth density data transmission with low-power consumption [2]. Currently, in many HPCs and datacenter networks, optical links composed of glass multimode fibers (MMFs) with a 50-μm diameter core have been already deployed, particularly in the rack-to-rack connections (less than 100 m). In these MMF links, the electrical signals are converted to optical signals at the board edges, while legacy copper wiring remains for on-board interconnections. Therefore, the next step and current research trends are in on-board optical interconnects, and thus, polymeric optical waveguides have been drawing much attention because of the ease of fabrication, good compatibility with printed circuit boards (PCBs), and low cost [3–5]. In order to meet the demand for complicated on-board wiring patterns, the ability to design wide variety of optical circuit patterns, such as core-crossing structures just in a single layer, is very important [6].

Over the last couple of years, extensive research has been done on multimode polymer optical waveguides with step-index (SI) cores [7–9]. Meanwhile, we have reported the advantages of graded-index (GI) core polymer waveguides for on-board interconnects: low propagation loss and low interchannel crosstalk. Furthermore, we have demonstrated that crossed polymer waveguides with multimode GI cores exhibit much lower loss at the intersections (crossings) than the conventional SI core counterpart [10]. In GI cores, the signal light is tightly confined near the core center due to the GI profile, so light leakage at the intersection is quite low compared to SI-core crossed waveguides.

Therefore, over the last a few years, several trials to fabricate GI core crossed polymer waveguides applying conventional photo-lithography techniques have been reported [11]. However, the refractive index profiles are not completely symmetrically parabolic forms, which is called semi-GI, so the crossing loss may not be reduced sufficiently. In addition, the photo-addressing method [12], the Mosquito method [13], and the laser writing method [14] have all been reported as methods for fabricating GI core multimode polymer optical waveguides. However, for the photo-addressing method, the applicable materials have been limited to poly norbornene. In the Mosquito method, it is difficult to form the core-crossing structures in just a single layer, and the laser writing method could have difficulty in achieving low loss and sufficiently high index contrast between the core and cladding.

In order to address these problems in fabricating low-loss crossed polymer waveguides, we have focused on the imprint method. In our previous results, the polymer optical waveguides with GI cores were fabricated by applying a UV curable acrylic resin with a low molecular-weight dopant [15]. In this case, although the acrylate resin had a three-dimensionally cross-linked structure to have a high thermal stability, the fabricated waveguides showed an index profile degradation even at room temperature in a couple of months. Even if a polymer matrix with high thermal stability were applied, we found such a

Optics EXPRESS

small molecular-weight (molecular size) dopant migrated, which degraded its concentration distribution [16]. Hence, the previous waveguides did not satisfy the solder-reflow resistance and reliability required for real applications of optical PCBs (O-PCBs).

Therefore, in this paper, a series of organic-inorganic hybrid resins whose high thermal resistance was already verified [17, 18] is applied to the imprint method. We expect no degradation in the GI profile after the monomers are cured, because the core and cladding monomers copolymerize to have rigid covalent bonds. In the following sections, we investigate the applicability of the organic-inorganic hybrid resin to the imprint method for low loss GI core polymer waveguides. Furthermore, we fabricate GI core optical waveguides with core-crossing structures, to experimentally confirm the great benefit of GI cores.

2. Fabrication for polymer optical waveguides using the imprint method

In Fig. 1, the fabrication procedure of the imprint method is schematically illustrated. The required properties for the materials in order to fabricate waveguides with GI cores using the imprint method are as follows: (1) monomers should be liquid and miscible so as not to cause phase separation after the mutual diffusion: (2) monomers for the core and cladding should copolymerize to have a strong chemical bonding and exhibit high heat resistance: (3) after curing, the core polymer should have a higher refractive index than the cladding by 0.01 to 0.03: (4) monomers should be photocurable: (5) the viscosity of the core material should be lower than 10,000 cP so as to fill the narrow grooves for the core easily. Organic-inorganic hybrid resins, SUNCONNECT®, supplied by Nissan Chemical Ind., Ltd. (core: NP-001, cladding: NP-208) are applied to the waveguides. The refractive index of the cladding material is 1.570, while 1.600 for the core material at 589.3-nm wavelength. The high thermal stability of the materials themselves is already reported by the material suppliers. Since the materials are three-dimensionally cross-linking, no glass transition temperature is observed. In addition, the TGA data shows that the temperature at which the degradation of the material begins is as high as 400 °C [17].

At first, the monomer for cladding is coated on a glass substrate, and the grooves for the core are formed on the under cladding by pressing a stamp mold made of poly dimethyl siloxane (PDMS) to the under-cladding monomer during UV curing. [Figs. 1(a) and 1(b)] The fabrication method for the PDMS mold, which has already been described in our previous article [15], is briefly introduced as follows: the PDMS mold is fabricated by replicating the relief pattern on a master mold (a rigid photo-resist on a silicon wafer substrate). Here, a negative photo-resist, TMMF S-2000 supplied by Tokyo Ohka Kogyo Co., Ltd. is used. Subsequently, a mixture of PDMS monomer and catalyst for cross-linking is casted over the master mold, followed by thermal curing to obtain the mold. After the under-cladding is cured, the PDMS mold is peeled off, and the grooves on the under cladding are filled with the liquid core monomer using a scalpel and UV cured. [Figs. 1(c) and 1(d)] Because of this procedure, a thin layer of the core could remain on the under-cladding, even if the excess core monomer is carefully eliminated. The residual core monomer makes a cross-linking of multiple cores aligned in parallel. However, we have already demonstrated in our previous article [15] that the core cross-linking structure shows small influence on the interchannel crosstalk in the case of GI core waveguides. Finally, the cladding monomer is coated over both the core and under-cladding to form the over-cladding. [Fig. 1(e)]

Here, the under-cladding and core are not completely cured at the steps of Figs. 1(b) and 1(d) before the over-cladding is coated and cured [Fig. 1(e)], during which the liquid state monomers can mutually diffuse to form concentration distributions. Similar diffusion takes place during the over-cladding formation, resulting in forming a symmetric GI profile. This monomer diffusion is a key process to control the GI profile. Furthermore, in order to take a sufficient diffusion time for monomers, an interim time is applied. The interim time is the time just after the over-cladding monomer is coated to the instant when the UV curing starts. During this procedure, if the under-cladding and cores are completely cured with a sufficient

Optics EXPRESS

UV curing time and no interim time, an SI profile could be formed using the same method and the same polymer materials.

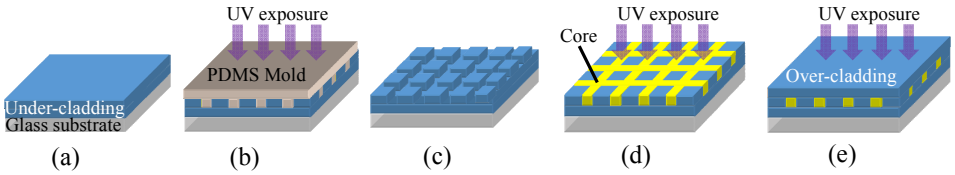

Fig. 1. Fabrication procedure of the imprint method.

Figure 2 shows the cross-sections of SI and GI core straight waveguides (no crossing structure) fabricated applying the imprint method. From Fig. 2, it is confirmed that a desired cores size of 40 × 40 μm are certainly formed with a 125-μm interchannel pitch in both SI and GI waveguides. Figure 3 shows the refractive index profile of the fabricated GI core measured using a two-beam interference microscope (Mizojiri Optics). From Fig. 3, gradual refractive index variation is observed, and its top is located at almost the core center. So, it is confirmed that the waveguide with an almost symmetric GI profile is fabricated by the imprint method, although there is a slight index bump at the boundary between over- and under-claddings. This index bump could be formed when the core monomer is coated on the under-cladding before it is completely cured. Because of the fabrication procedure particular to the imprint method, such a thin layer with an index bump between over- and under-claddings is likely to remain even in SI core waveguides, which is found in the cross-sections in Fig. 2. Since this bump has a higher index than the cladding, an excess interchannel crosstalk due to the cross-linking by the high-index layer is a concern. However, in our previous report [12], we already confirmed that such a cross-linking structure showed little effect on the crosstalk in GI core waveguides because of the tight light confinement effect of GI profiles, which is one of the advantages of GI core waveguides fabricated using the imprint method.

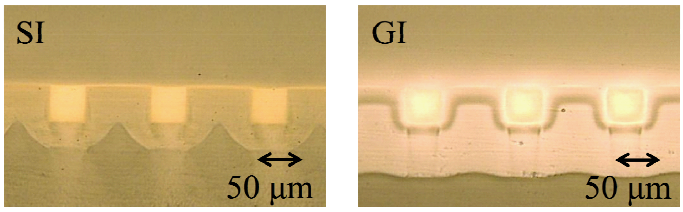

Fig. 2. Cross-section of the fabricated waveguides.

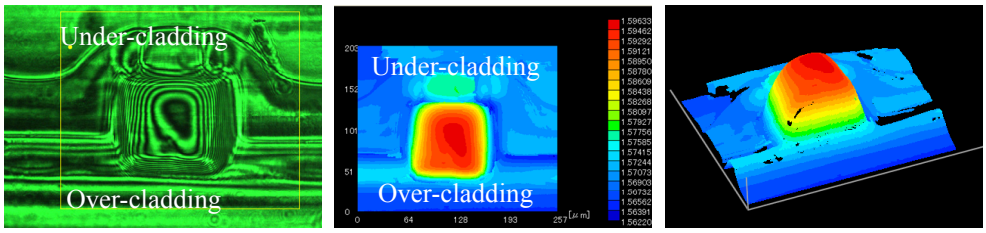

Fig. 3. Observed (a) interference fringe (b) 2D refractive index profile (c) 3D refractive index profile in a fabricated GI waveguide.

Optics EXPRESS

3. Crossed polymer optical waveguides

3.1 Fabrication for crossed waveguides

In the imprint method, not only straight wiring patterns but also various patterns such as crossing and bending patterns can be formed. Therefore, SI core and GI core crossed waveguides are fabricated using the imprint method with the same materials. First, crossing patterns are designed. Figure 4 shows a schematic top view of the designed crossed waveguide, and Table 1 shows the parameters for the design. In order to investigate the dependence of crossing loss on the number of crosses, the number of crossed cores is varied from 0 to 50 in increments of 5. In the first several crossings, the high-order modes which have strong optical fields near the core-cladding boundary preferentially leak out at the intersection, so the loss tends to increase nonlinearly with respect to the number of crossings. Therefore, when the number of crossings is small, the loss per crossing is not a robust measure. In order to avoid this problem in our measurements, the number of crossings involved in the waveguides is as large as 50. Meanwhile, the cross angle varies at 30, 45, 60 and 90-degrees in order to investigate the cross-angle dependence. The interchannel pitch is 125-μm in both axial and lateral directions.

Figure 5 shows the top-views of the fabricated crossed waveguides with various cross angles. As shown in Fig. 5, there is no structural defect in all the waveguides, and it is found that the waveguides perfectly duplicate the designed patterns. The cross-sections of the SI and GI crossed cores with a cross angle of 90 degree under various numbers of crossing are shown in Figs. 6 and 7, respectively. Although these cross-sections are just observed by a microscope, it is obvious that the SI cores after 50 crossings are remarkably dark in Fig. 6(c), from which high crossing loss in SI core waveguides are confirmed visually.

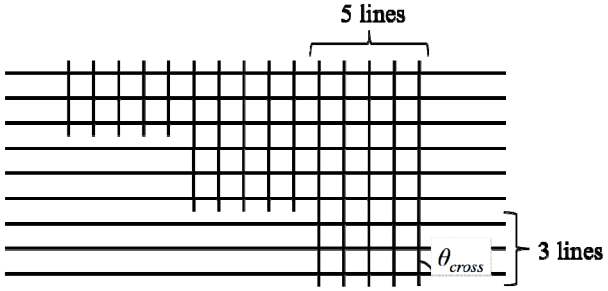

Fig. 4. Schematic top view of a designed crossed pattern.

Table 1. Designed parameters for crossed waveguide

Number of crossings	0 - 50
Cross angle: θ_{cross}	30°, 45°, 60°, 90°
Core size	40 μm × 40 μm
Interchannel pitch	125 μm
Refractive index profile	SI, GI

Optics EXPRESS

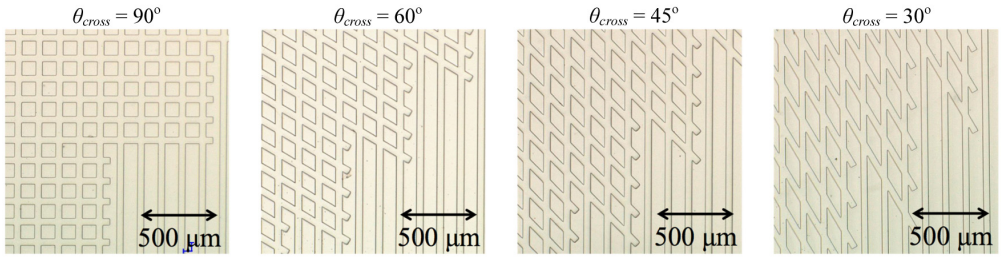

Fig. 5. Top-views of the fabricated crossed waveguides.

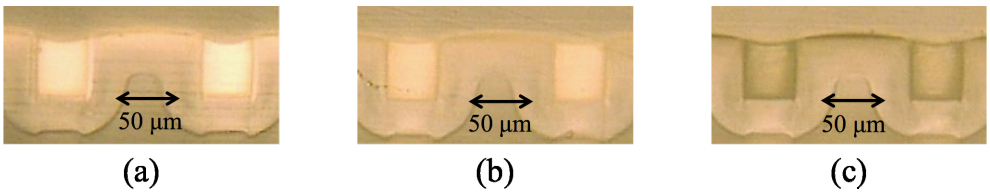

Fig. 6. Cross-sections of the fabricated SI core after (a) no crossing (b) 10 crossings (c) 50 crossings.

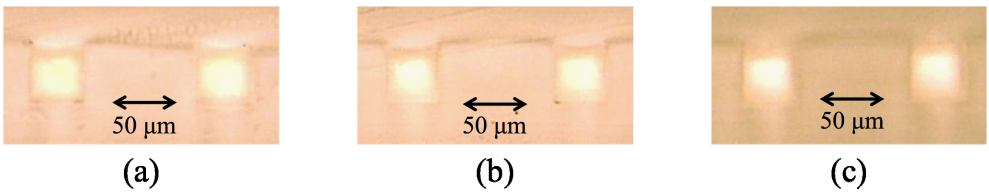

Fig. 7. Cross sections of the fabricated GI cores after (a) no crossing (b) 10 crossings (c) 50 crossings.

3.2 Insertion loss of crossed waveguides

Insertion losses of the crossed waveguides are measured under two different conditions. One is using a 1-m long single-mode fiber (SMF) and 200-μm core SI multimode fiber (MMF) as the launch and detection probes, respectively, as shown in Fig. 8(a). On the other hand, 1-m long 50-μm core GI-MMFs are used for both launch and detection probes, as a more realistic condition for on-board applications of waveguides, as shown in Fig. 8(b). Under both conditions, a VCSEL emitting at 850-nm wavelength is used as the light source. Figure 9 shows the near-field pattern (NFP) and calculated encircled flux (EF) of the 50-μm core GI-MMF probe. The EF satisfies the specification of the MMF link for 10 GB Ethernet (10GBASE-SR). Figure 10 shows the NFPs of the fabricated SI and GI core crossed waveguides with no core crossings (straight). A 1-m long SMF is used for the launch probe to couple the light to the core with a small spot size. In the SI core waveguide, the output optical field spreads out to the entire core, while the small spot size of the launch beam is maintained in the GI core waveguide, due to strong optical confinement.

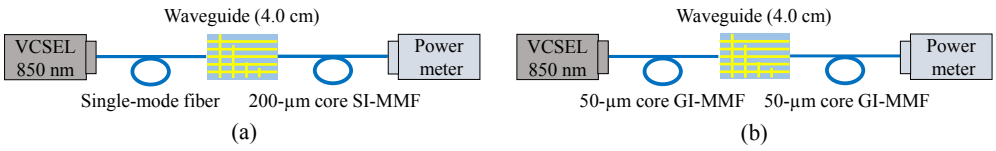

Fig. 8. Schematic diagrams of insertion loss measurement setup (a) condition A (b) condition B.

Optics EXPRESS

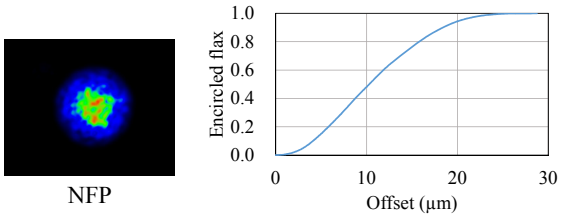

Fig. 9. NFP and EF of the 1-m long 50-μm core GI-MMF probe.

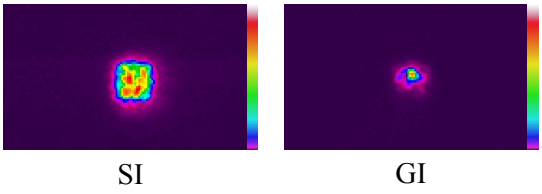

Fig. 10. NFPs of fabricated waveguides with no core crossing (straight).

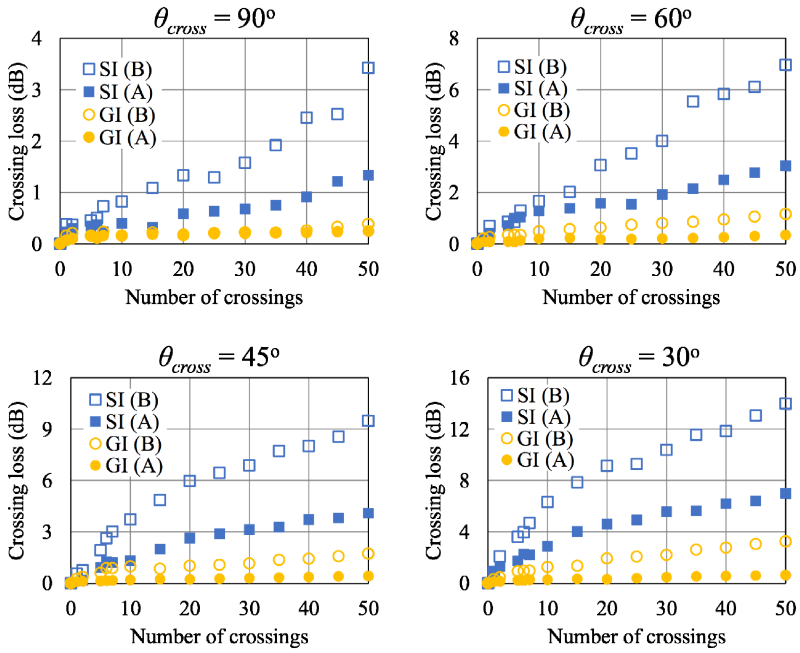

Fig. 11. Loss dependence on the crossing number in fabricated crossed waveguides.

The crossing loss of the waveguides with cross angles from 30 to 90 degrees are shown in Fig. 11. The losses shown in this paper are the average values of the 3 channels with the same structure, as described in the waveguide design (Fig. 4). The loss values are obtained by subtracting the insertion loss of the straight waveguide with the same length from the insertion losses of the crossed waveguide. The insertion losses of the SI-core and GI-core straight waveguides under measurement condition A are 1.26 dB and 0.546 dB, respectively, and 2.95 dB and 1.61 dB, respectively, under measurement condition B. These values are used as references to calculate the crossing loss. The insertion loss consists of the coupling losses with the probe fibers, the propagation loss of the waveguide, and the crossing loss caused by the light leakage to unwanted directions at the intersections. From Fig. 11, it is found that the SI-core shows higher loss in all the cross angles and number of crossings. In

Optics EXPRESS

the SI-core, as the number of crossing increases, the crossing loss increases continuously, up to 50 crossings, and when θ_{cross} = 90°, the loss per cross estimated from the slope is 0.0254 dB under condition (A) which could be the mildest condition. In addition, when θ_{cross} = 30°, the estimated loss per cross increases to 0.3244 dB under condition (B), the most severe condition. On the other hand, in the GI-core, the crossing loss increases with a gentle slope with respect to the number of crossings, and even when θ_{cross} = 90°, the losses per cross under conditions (A) and (B) are as low as 0.0063 dB and 0.0078 dB, respectively. Thus, GI-cores in crossed waveguides can decrease the crossing loss by almost one fourth of the loss in SI-core crossed waveguides. Both SI-core and GI-core waveguides show higher loss under measurement condition B than under the measurement condition A. This is because the optical power is coupled to the high order modes in the waveguides whose optical power mainly exists near the core-cladding boundary. Hence, at the intersection, these higher-order modes are likely to leak than the lower order modes which are tightly confined near the core center. However, in the SI-core, the crossing loss sharply increases under both conditions, whereas the GI-core shows a gentle slope of the loss increment with respect to the crossing number, even under measurement condition B, due to tight optical confinement. Other research group reported that a GI-core cross waveguide with a cross angle of 90° fabricated using the photo-addressing method exhibited a loss per cross of 0.0028 dB [12] under condition (B). The slightly higher crossing loss observed in GI-core crossed waveguide fabricated in this paper could be attributed to the index profile. As we already theoretically showed in [10] that the crossing loss is sensitive to the index profile.

Next, the crossing losses after passing 50 crossings under different cross angles (from 30 to 90-degrees) are summarized in Fig. 12(a). As shown in Fig. 12(a), the GI-core waveguide shows consistently lower loss than the SI-core at all the cross angles. Furthermore, it is found that in the GI-core waveguide, the crossing loss is almost independent of the cross angle. This is because the light leakage at the intersection is reduced remarkably due to the strong light confinement effect of the GI profile.

On the other hand, in the SI-core, higher crossing loss is observed with decreasing the cross angle. This is because the volume of the intersection of two cores increases with decreasing the cross angle. Since in SI core waveguides, the light propagates with the total internal reflection scheme, the leakage of light also increases as the volume of the intersection increases. Under the worst case condition (B), the loss in the SI-core crossed waveguide is as high as 14 dB, which is almost five times higher than the loss in the GI-core counterpart under the same worst condition.

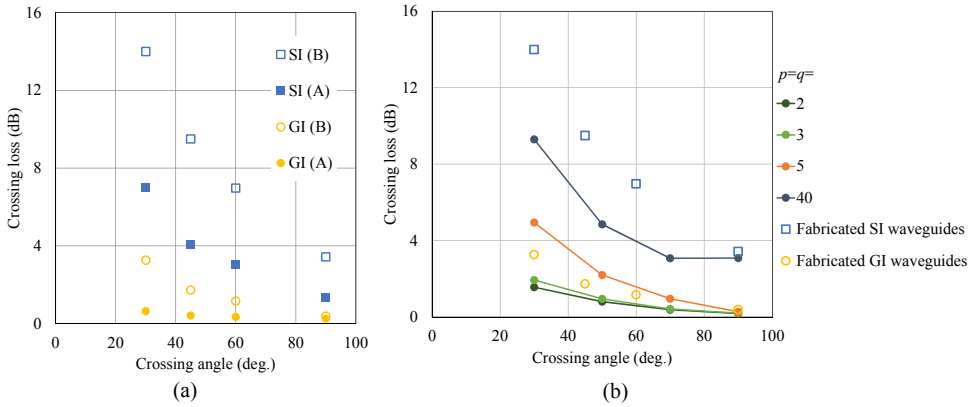

Fig. 12. Cross angle dependence of the loss after 50 crossings (a) in fabricated waveguides and (b) comparison with the simulated results [10].

Optics EXPRESS

In Fig. 12(b), the measured results are compared to the simulated results we previously reported in [10]. In this simulation, we assume a launch condition using a 50-μm GI core MMF probe. As mentioned above, the crossing loss is sensitive to the refractive index profile, so in the simulation, the index profile dependence of the crossing loss was investigated in detail. Here, the refractive index profile was approximated by Eqs. (1)-(4).

$$n(x,y) = n_{co}\left[1-2\Delta\{f(x)+g(y)\}\right]^{\frac{1}{2}} \tag{1}$$

$$f(x) = \left|\frac{x}{a_x}\right|^p, \quad g(y) = \left|\frac{y}{a_y}\right|^q, \quad \Delta = \frac{n_{co}^2 - n_{cl}^2}{2n_{co}} \tag{2}$$

$$f(x)+g(y) \geq 1 \tag{3}$$

$$n(x,y) = n_{cl} \tag{4}$$

Here, n_{co} and n_{cl} are the refractive indices at the core center and the cladding, respectively, while *ax* and *ay* are the half-width and the half-height of the rectangular core, respectively. Two index exponents, *p* and *q* express the index profiles in the horizontal and vertical directions in the core, respectively. All the intersections are assumed to have an SI profile with the same refractive index as the core center, which should be the worst case for the GI-core crossed waveguide [10].

In Fig. 12(b), the results when $p = q = 2$, 3, 5, and 40 are shown to estimate the index profiles actually formed in the fabricated waveguides. From the result, the SI core could be approximated with $p = q = 40$ or rather higher value, while the GI core could correspond to $p = q = 4$ to 5. From the measured index profiles using the two-beam interference microscope, the index exponents *p* and *q* are estimated to 2.4 and 2.2, respectively. It is noted that the experimentally measured loss in Fig. 12(b) is less dependent on the cross angle, which is a similar tendency to the loss when $p = q = 2$ to 3. Hence, the excess loss observed in the fabricated GI core waveguide compared to the simulated results with $p = q = 2$ and 3 could be caused by a deviation of index profile from the approximated forms by Eqs. (1)-(4).

4. Thermal resistance of polymer optical waveguides

4.1 Solder-reflow resistance test

The thermal resistance of GI core *straight* waveguides fabricated using the organic-inorganic hybrid resin, SUNCONNECT® is investigated. Assuming the solder-reflow process, the resistant test is carried out under 250 °C for 1 minute in a heat bath. The insertion loss before and after the resistant test is measured and compared using a setup similar to Fig, 8(a). Here, previous waveguides composed of an acrylic resin with dopant [12] are also tested for comparison. Both waveguide samples are fabricated using the imprint method. Figure 13 shows the measured insertion loss before and after the test. The insertion loss of the acrylic resin based waveguide increases about 1 dB from 0.70 dB to 1. 56 dB after the test, despite such a very short waveguide (4-cm long). On the other hand, the insertion loss of the organic-inorganic hybrid resin based waveguide shows almost no increment. From these results, it is confirmed that the waveguide fabricated using the organic-inorganic hybrid resin based waveguides has solder-reflow capability.

Optics EXPRESS

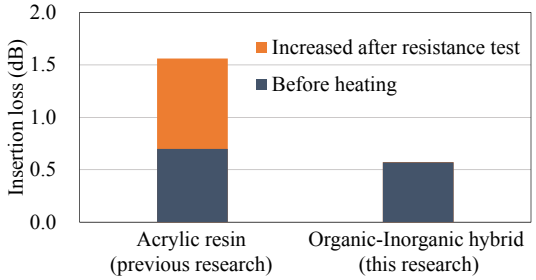

Fig. 13. Insertion losses of straight waveguides fabricated using the imprint method before and after thermal resistant test assuming a solder-reflow process.

4.2 High temperature/high humidity test

We evaluate the high temperature stability and long-term reliability of the waveguides by applying the waveguide samples to aging test. The aging test is carried out under high temperature/high humidity atmosphere (85 °C/85%RH) for 1000 hours, and tested sample is the GI-core crossed waveguide (cross angle: 90°). The insertion loss of the waveguides before and after the aging test is measured using the same setup as Fig. 8(a). Figure 14 shows the insertion loss before and after the aging test. From Fig. 14, the estimated loss per cross of before and after testing are 0.0063 dB and 0.0064 dB, respectively. Thus, it is confirmed that the insertion loss increment is negligible even after 1000–hour aging, and it is obvious that the waveguide using the organic-inorganic hybrid resin has high thermal stability and long-term reliability.

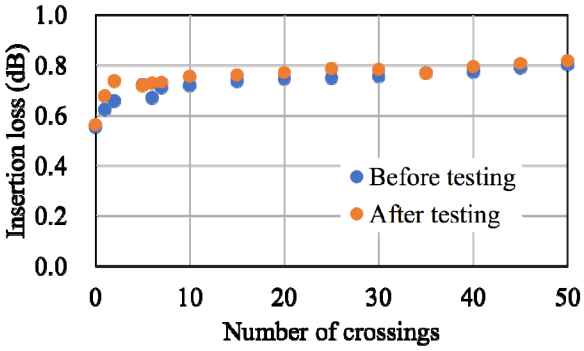

Fig. 14. Insertion losses of a straight GI waveguide before and after heating.

5. Conclusion

In this paper, we applied a series of organic-inorganic hybrid resins, SUNCONNECT® with thermal resistance to the imprint method and succeeded in fabricating low-loss crossed waveguides with GI cores that exhibit solder-reflow capability. The obtained GI crossed waveguide shows a crossing loss of 0.0063 dB/cross and it is lower than the results previously reported [11], which is achieved by forming asymmetric index profile. Another great advantage of these waveguides is to exhibit low crossing losses over a wide range of cross angles. Furthermore, high temperature/high humidity test was conducted on the obtained waveguides, the insertion loss almost no increase was observed even after 1000 hours, so it was confirmed that the waveguide had high reliability.

It is revealed that GI-core polymer waveguides play a key role for realizing high-density O-PCBs just applying the imprint method.